A

```
  1 MRMSVGLSLL LPLWGRTFLL LLSVVMAQSH WPSEPSEAVR DWENQLEASM HSVLSDLHEA
 61 VPTVVGIPDG TAVVGRSFRV TIPTDLIASS GDIIKVSAAG KEALPSWLHW DSQSHTLEGL
121 PLDTDKGVHY ISVSATRLGA NGSHIPQTSS VFSIEVYPED HSDLQSVRTA SPDPGEVVSS
181 ACAADEPVTV LTVILDADLT KMTPKQRIDL LHRMRSFSEV ELHNMKLVPV VNNRLFDMSA
241 FMAGPGNPKK VVENGALLSW KLGCSLNQNS VPDIHGVEAP AREGAMSAQL GYPVVGWHIA
301 NKKPPLPKRV RRQIHATPTP VTAIGPPTTA IQEPPSRIVP TPTSPAIAPP TETMAPPVRD
361 PVPGKPTVTI RTRGAIIQTP TLGPIQPTRV SEAGTTVPGQ IRPTMTIPGY VEPTAVATPP
421 TTTTKKPRVS TPKPATPSTD STTTTTRRPT KKPRTPRPVP RVTTKVSITR LETASPPTRI
481 RTTTSGVPRG GEPNQRPELK NHIDRVDAWV GTYFEVKIPS DTFYDHEDTT TDKLKLTLKL
541 REQQLVGEKS WVQFNSNSQL MYGLPDSSHV GKHEYFMHAT DKGGLSAVDA FEIHVHRRPQ
601 GDRAPARFKA KFVGDPALVL NDIHKKIALV KKLAFAFGDR NCSTITLQNI TRG
```

B

name	peptide
(mucin-like domain of α-DG)	
316-337	ATPTPVTAIGPPTTAIQEPPSR
336-355	SRIVPTPTSPAIAPPTETMA
364-383	GKPTVTIRTRGAIIQTPTLG
385-403	IQPTRVSEAGTTVPGQIRP
401-420	IRPTMTIPGYVEPTAVATPP
418-440	TPPTTTTKKPRVSTPKPATPSTD
435-454	ATPSTDSTTTTTRRPTKKPR
451-470	KKPRTPRPVPRVTTKVSITR
469-488	ITRLETASPPTRIRTTTSGVP
(mucin tandem-repeat region)	
MUC1	AHGVTSAPDTRPPPGSTAPP
MUC2	PTTTPITTTTTVTPTPTPTGTQT
MUC3	HSTPSFTSSITTTETTS
MUC4	ATPLPVTDTSSASTGH
MUC7	TTAAPPTPSATTPAPPSSSAPPE
MUC11	SGLSEESTTSHSSPGSTHTT
MUC20	SSESSASSDGPHPVITPSR

FIGURE 1. **Sequences of acceptor peptides.** *A*, amino acid sequence of human DG. Amino acids are indicated by the single-letter amino acid codes. The mucin-like domain (316–489) is indicated by *boldface*. The *underlines* indicate acceptor peptides. *Dashed line* indicates a signal sequence. *B*, summary of acceptor peptides from mucin-like domain of α-DG and mucin tandem repeat region.

(1 × 100 mm; GL Sciences Inc., Tokyo) with a model 1100 series liquid chromatography system (Agilent Technologies, Waldbronn, Germany). Mannosyl peptides were eluted at a flow rate of 20 μl/min using a linear gradient of 0–50% solvent B, where solvents A and B were 0.085% (v/v) aqueous trifluoroacetic acid and 0.075% (v/v) trifluoroacetic acid in 80% (v/v) acetonitrile, respectively. Three peptides thus obtained were subjected to Edman degradation using a Procise HT protein sequencing system (Applied Biosystems, Foster City, CA). "Cart pulsed liquid" and "Flask normal" were used for default programs of reaction and conversion cycle, respectively. At proline residues (3rd, 8th and 13th), the "Cart PL Proline" program was used for reaction cycles. Except for 8-mm peptide supports (Beckman Coulter Inc., Fullerton, CA), all sequence programs and reagents were supplied by Applied Biosystems. To reduce chemicals and background peaks, the chromatogram of the previous cycle was subtracted from one of the current cycle with the 610A data analysis system (Applied Biosystems) using the "Subtraction Mode". To identify mannosyl-threonyl residue, 100 pmol of synthetic mannosyl-threonine was subject to protein sequencer. The peaks of 3-phenyl-2-thiohydantoin-mannosyl-threonine and related molecule were eluted on the first cycle of the sequencer. A MALDI-TOF mass spectrum was obtained on a Ultraflex mass spectrometer (Bruker Daltonics, Bremen, Germany) in a reflector mode using 2,5-dihydroxybenzoic acid as a matrix. For MS/MS spectra, parent ion was selected ± 15 Da from the observed MH^+ value using time gate and re-accelerated (LIFT mode).

RESULTS

Detection of POMT Activity against Various Peptides—We previously detected POMT activity when POMT1 and POMT2 were co-expressed in human embryonic kidney 293T cells using glutathione *S*-transferase-α-DG as an acceptor (6). In the present study, we examined whether or not synthetic peptides worked as an acceptor. We prepared nine ~20-amino acid peptides that covered the mucin-like domain of α-DG (Fig. 1). When we measured the POMT activity using these peptides, these peptides were mannosylated to different degrees. The peptide sequence 401–420 worked as a prominent acceptor, followed by the peptide sequence 336–355 (Fig. 2). The POMT activity was 4.03 pmol/h/mg total protein against peptide 401–420 and 2.32 pmol/h/mg total protein against peptide 336–355. The POMT activities against the other peptides were less than peptide 401–420 and 336–355 (<0.63 pmol/h/mg total protein), suggesting the occurrence of α-DG peptide-specific *O*-mannosylation.

Mucin type *O*-linked glycosylation is initiated by the action of a family of UDP-GalNAc, polypeptides *N*-acetylgalactosaminyltransferase (pp-GalNAc-T), which catalyze the transfer of GalNAc from the nucleotide sugar UDP-GalNAc to the hydroxyl group of either Ser or Thr. Peptides derived from the tandem repeat region of mucins, which have a high density of Ser/Thr, were utilized efficiently by all pp-GalNAc-Ts (19). Therefore, we examined whether or not several peptides of mucin tandem repeat regions worked as an acceptor of *O*-mannosylation (Fig. 1*B*). Among these peptides, MUC2 and MUC3 showed slight POMT activities (0.7 and 0.49 pmol/h/mg total protein, respectively). These results indicated that mucin peptides worked as poor acceptors for

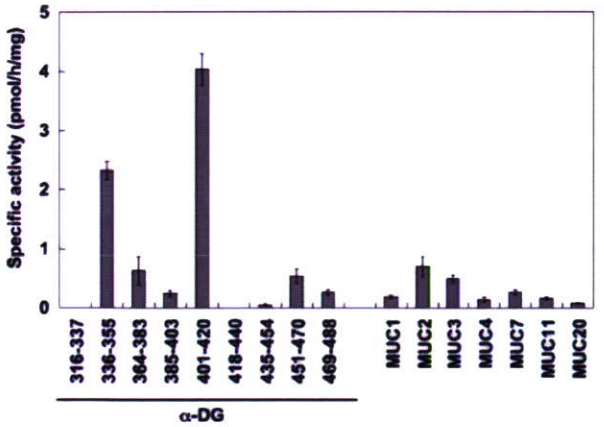

FIGURE 2. **POMT activities against various peptides.** POMT activity was measured in a 20-μl reaction volume containing 20 mM Tris-HCl, pH 8.0, 100 nM mannosylphosphoryldolichol (125,000 dpm/pmol), 2 mM dithiothreitol, 10 mM EDTA, 0.5% *n*-octyl-β-D-thioglucoside, 1 mM synthetic peptide, and 40 μg of microsomal membrane fraction. After incubation at 25 °C for 1 h, the peptide was separated by reversed-phase HPLC, and then the incorporation of [^{3}H]mannose was measured with a liquid scintillation counter. Average values ±S.D. of three independent experiments are shown.

TABLE 1

Kinetics analysis of POMT activity against various peptides

The kinetic parameters were analyzed by means of Hanes-Woolf plotting (as shown in supplemental Fig. S1) based on the POMT reactions performed using various substrate concentrations, 0.25–4 mM of the acceptor peptide.

Peptide	K_m	V_{max}	K_m/V_{max}
	mM	*pmol/h/mg*	
336–355	0.63	3.98	0.16
364–383	9.70	3.98	2.44
385–403	2.96	0.70	4.23
401–420	0.73	7.11	0.10
451–470	2.98	1.82	1.64
MUC2	4.00	2.97	1.34
MUC3	2.11	1.39	1.52

O-mannosylation, suggesting that there are preferred protein sequences for *O*-mannosylation.

Kinetics Analysis of POMT Activity against Various Peptides—Among seven peptides (peptides 336–355, 364–383, 385–403, 401–420, 451–470, MUC2, and MUC3) examined, peptides 336–355 and 401–420 had the lowest K_m values (0.63 and 0.73 mM, respectively) (Table 1 and supplemental Fig. S1). The K_m/V_{max} values for peptides 336–355 and 401–420 were 0.16 and 0.10, respectively, and the K_m/V_{max} values for other peptides were 8 times higher than that of peptide 336–355. These results suggest that the affinities of POMT for peptides 336–355 and 401–420 are comparable and that peptides 336–355 and 401–420 are the most suitable acceptors for POMT reaction under these experimental conditions.

Substrate Specificities and Effect of Change of Amino Acids of Peptides—Peptide 336–355 and peptide 401–420 have six and four potential *O*-mannosylated Ser and Thr residues, respectively (Fig. 1*B*). To elucidate which Ser or Thr was preferentially modified by *O*-mannosylation, each Ser or Thr of the peptides was changed to Ala one by one and then the *O*-mannosylation efficiencies of the mutated peptides were examined. Six mutated peptides were prepared from peptide 336–355 and four peptides were prepared from peptide 401–420 (Fig. 3*A*). For peptide 336–355, changing Ser-336 or Ser-344 to Ala did not affect the acceptor efficiency of the peptides, whereas

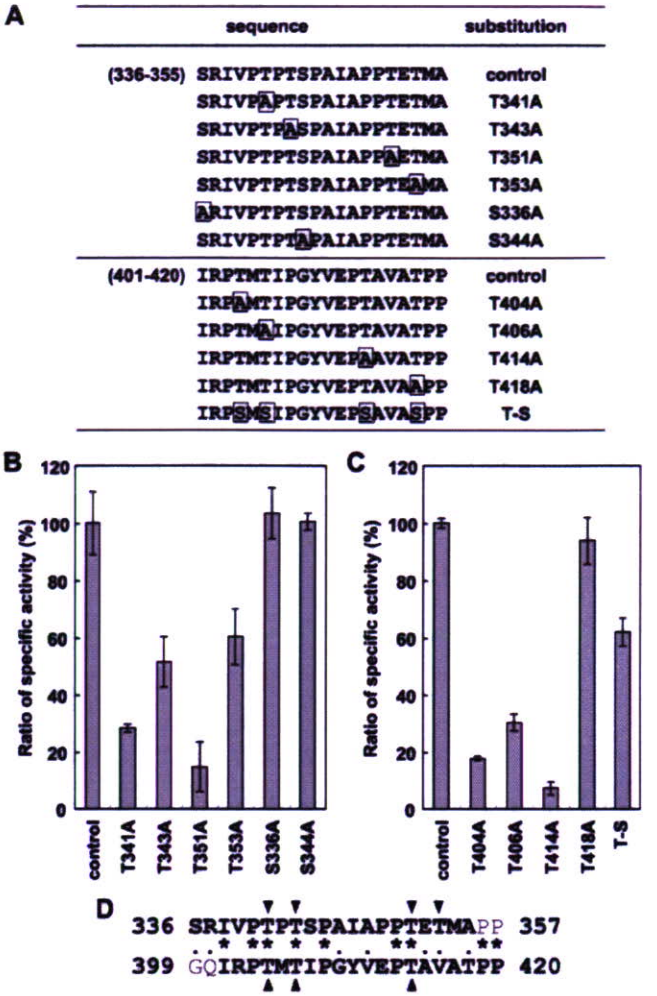

FIGURE 3. **Effect of substitution of amino acids of peptides.** *A*, summary of the peptides 336–355 and 401–420 in which *boxed* A and S residues indicate substitutions for Thr. *B* and *C*, relative activities of the mutated peptide 336–355 (*B*) and peptide 401–420 (*C*) were evaluated by the POMT reactions using 1 mM acceptor peptide. Average values ±S.D. of three independent experiments are shown. *D*, alignment of peptides 336–355 and 401–420 was generated by the GENETYX-Mac program (GENETYX Corp., Tokyo, Japan) based on Lipman-Pearson's method. The *asterisks* indicate identical amino acids, and the *dots* indicate similar amino acids. The *arrowheads* indicate Thr residues whose substitution reduced the POMT activity. Residues shown in *nonbold* are residues flanking the peptides.

changing Thr-341 or Thr-351 to Ala greatly reduced the acceptor efficiency (by 71.7 and 85.1%, respectively) and changing Thr-343 or Thr-353 to Ala moderately reduced the acceptor efficiency (by 48.5 and 39.8%, respectively) (Fig. 3*B*). For peptide 401–420, changing Thr-418 to Ala slightly affected the acceptor efficiency, whereas changing Thr-404, Thr-406, or Thr-414 to Ala greatly reduced the acceptor efficiency (by 82.3, 69.7, and 92.7%, respectively) (Fig. 3*C*). The results indicate that Thr-351 of peptide 336–355 and Thr-414 of peptide 401–420 were prominently modified by *O*-mannosylation. Next, to elucidate the preference of *O*-mannosylation of Ser and Thr residues, four Thr residues of peptide 401–420 were changed to Ser (Fig. 3*A*, *peptide T-S*) and then the *O*-mannosylation efficiency of peptide T-S was examined. Changing Thr to Ser reduced the acceptor efficiency by 62.2% (Fig. 3*C*). This result indicates that

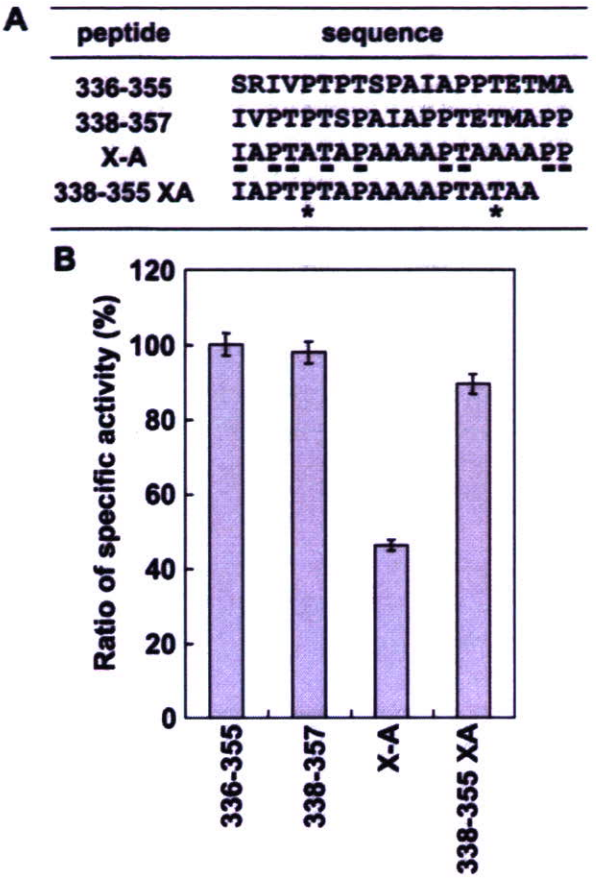

FIGURE 4. **Sequence of preferential acceptor peptide for POMT.** *A*, summary of the acceptor peptides. The *underlines* indicate identical amino acids between peptide 336–355 and peptide 401–420 as shown in Fig. 3*D*. The *asterisks* indicate the reverted Ala to Pro-342 and Thr-353. *B*, relative activities were evaluated by the POMT reactions using 1 mM acceptor peptide. Average values ±S.D. of three independent experiments are shown.

the POMT *O*-mannosylates both Thr and Ser but prefers Thr to Ser.

Interestingly, peptides 336–355 and 401–420 have similar sequences. In an alignment analysis of these peptides and adjacent amino acid residues (Fig. 3*D*), the two sequences have nine identical amino acids (indicated by *asterisks*) and seven similar amino acids (indicated by *dots*). Taken together, these results indicate that the similar *O*-mannosylation efficiencies of the two peptides are due to the similarity of their sequences.

Next, we tried to identify a consensus sequence for *O*-mannosylation. First, to examine the necessity of C-terminal Pro-Pro and N-terminal Ser-Arg, we prepared peptide 338–357 (Fig. 4*A*). The POMT activity against peptide 338–357 was almost the same as the activity against peptide 336–355 (by 97.8%) (Fig. 4*B*). This result indicates that the C-terminal Pro-Pro and N-terminal Ser-Arg have a negligible effect on *O*-mannosylation efficiency. Then we examined the contribution of nonidentical amino acids between peptides 336–355 and 401–420 on *O*-mannosylation. To address this question, we prepared peptide *X*-A in which Ala was substituted for all nonidentical amino acids (Fig. 4*A*). The mutated peptide *X*-A reduced the acceptor efficiency by 46.2% (Fig. 4*B*), suggesting that nonidentical amino acids also are important for efficient *O*-mannosylation. Then we prepared the peptide 338–355 *X*A in which Ala-342 was reverted to Pro and Ala-353 was reverted to Thr (indicated by *asterisks*). The reverted peptide 338–355 *X*A restored the acceptor efficiency to 89.3% of peptide 336–355. Taken together, these results suggest that the identical amino acid sequence between peptide 401–420 and peptide 336–355 is necessary for efficient *O*-mannosylation and that (I*X*PT(P/*X*)T*X*P*XXXX*PT*X*(T/*X*)*XX*) is a consensus sequence for *O*-mannosylation.

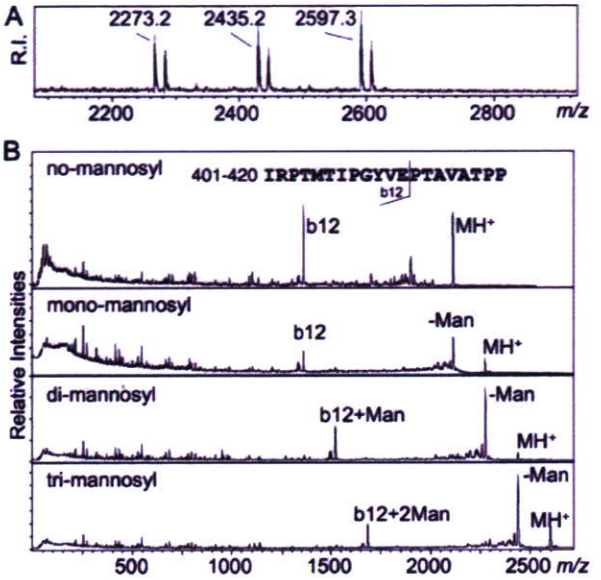

FIGURE 5. **MALDI-TOF MS and MS/MS spectra of mannosyl peptides.** *A*, MS spectrum of Con A-purified mannosyl peptides. Due to oxidation of the methionyl residue, +16-Da peaks were detected (*m/z* 2289.2, 2451.2, and 2613.3). *B*, MS/MS spectra of non-, mono-, di-, and tri-mannosylated peptides. The calculated average mass value of b12 fragment ion is 1359.6. Each observed mass = *m/z* (b12)1360.2 (*non-mannosyl* spectrum), 1361.1 (*mono-mannosyl* spectrum), (b12+Man)522.6 (*di-mannosyl* spectrum), (b12+2Man)1684.5 (*tri-mannosyl* spectrum).

MALDI-TOF MS Analysis and Edman Degradation Analysis—The enzymatic products of peptide 401–420 were analyzed by MALDI-TOF MS and Edman degradation to determine the number of attached mannose residues and their sites of attachment. The mannosylated peptides from the POMT reaction using peptide 401–420 as an acceptor were purified by Con A-Sepharose column followed by reversed-phase HPLC. The POMT reaction mixture showed several peaks around 22~23 min (supplemental Fig. S2*A*). A large peak at 23 min derived from the original peptide 401–420 was obtained from the unbound fraction of the Con A-Sepharose column (supplemental Fig. S2*B*, indicated by *closed triangle*). Three peaks around 22–23 min recovered from the bound fraction of the Con A-Sepharose column appear to be mannosyl peptides (supplemental Fig. S2*C*, indicated by *open triangle*).

The purified mannosylated peptides were subjected to MS analysis (Fig. 5). The monoisotoic mass value calculated from the peptide 401–420 is 2111.1 for $(M+H)^+$. On the other hand, the spectrum of the products showed three *m/z* values for $(M+H)^+$ of 2597.3, 2435.2, and 2273.2, suggesting that three, two, and one mannosyl residues have been transferred to the peptide, respectively (Fig. 5*A*). Then each peak was subjected to

MS/MS analysis to determine the sites of attachment by mannose. MS/MS with selection of the ion at m/z 2597 resulted in detection of a demannosylated ion m/z 2438 (peptide 401–420 + 2Man) and b-series ion m/z 1685 (b12, peptide 401–412 + 2Man). MS/MS with selection of the ion at m/z 2435 resulted in detection of ions m/z 2274 (peptide 401–420 + Man) and m/z 1522 (b12, peptide 401–412 + Man). MS/MS with selection of the ion at m/z 2273 resulted in detection of ions m/z 2113 (peptide 401–420) and m/z 1358 (b12, peptide 401–412) (Fig. 5*B*). These results indicated that the POMT enzymatic products of peptide 401–420 have three, two, and one Man residues.

Analysis of the amino acid sequences of these mannosylated peptides to determine the mannosylated Thr residues (supplemental Fig. S3) showed that the mono-mannosylated peptide was mannosylated mainly at Thr-414 and slightly at Thr-404 and Thr-406, the di-mannosylated peptide was mannosylated at Thr-406 and Thr-414, and the tri-mannosylated peptide was mannosylated at Thr-404, Thr-406, and Thr-414. These results indicate that 1) Thr-414 was the residue that was most frequently modified by *O*-mannosylation, 2) Thr-404 and Thr-406 were sequentially mannosylated after Thr-414, and 3) Thr 418 was not mannosylated. To confirm the conclusions, we performed a time course study of *O*-mannosylation. As shown in supplemental Fig. S4, mono-mannosylated peptide appeared at the early stage of the reaction (~15 min), and then the amount of di- and tri-mannosylated peptides increased at later stages. Taken together, these results indicate that *O*-mannosylation did not occur at random but occurred sequentially.

Effect of Mannosylation of Thr-414 on Substrate Efficiency—To examine whether the presence of mannose on the peptide affects *O*-mannosylation efficiency, we synthesized a mono-mannosyl peptide (IRPTMTIPGYVEPT(Man)AVATPP, named as peptide 401–420(T414Man)) and compared kinetic parameters with peptide 401–420 (supplemental Fig. S5). The K_m value for peptide 401–420(T414Man) (0.01 mM) was remarkably lower than that of peptide 401–420 (0.73 mM), and the V_{max} value for peptide 401–420(T414Man) (9.63 pmol/h/mg) was higher than that of peptide 401–420 (7.11 pmol/h/mg). These results indicate that the mannosylation of Thr-414 in peptide 401–420 facilitates subsequent mannosylation.

DISCUSSION

In this study, we identified a preferred amino acid sequence for mammalian *O*-mannosylation using a series of synthetic peptides whose sequences were derived from the mucin-like domain of human α-DG. Our data show that the peptide sequences 336–355 and 401–420 from α-DG are suitable acceptors for *O*-mannosylation, whereas other sequences including various mucin tandem repeat regions were poor acceptors. Interestingly, peptides 336–355 and 401–420 had very similar amino acid sequences and had comparable K_m values. These findings suggest that these peptides have the same affinity for POMT and have what appears to be a consensus sequence (I*X*PT(P/*X*)T*X*P*XXXX*PT*X*(T/*X*)*XX*) for mammalian *O*-mannosylation. The positions of Pro and Thr residues in the two peptides are especially similar. A BLAST search for proteins with this sequence turned up only α-DG, suggesting that the primal *O*-mannosylated protein is α-DG.

We found that Thr residues modified by *O*-mannosylation in the peptides 336–355 and 401–420 were mannosylated sequentially rather than at random. The substitution analysis showed that Thr-341, Thr-343, Thr-351, and Thr-353 of peptide 336–355 and Thr-404, Thr-406, and Thr-414 of peptide 401–420 are mannosylated (Fig. 3). Interestingly, the effectiveness of substituted Thr depended on the position; the third Thr residues from the N terminus of these peptides (Thr-351 and Thr-414) were most effective, followed by the first Thr residues (Thr-341 and Thr-404) and then the second Thr residues (Thr-343 and Thr-406). These results indicate that three Thr residues in the consensus sequence are necessary for *O*-mannosylation. Because the third and first Thr residues in the peptides 336–355 and 401–420 are located next to a Pro residue, POMT may prefer a PT motif as an acceptor. The result that the acceptor efficiency of peptide 338–355 *X*A is higher than that of peptide *X*-A (Fig. 4) also suggests the presence of a PT motif is necessary for preferential *O*-mannosylation. However, the PT motif by itself does not seem to be enough for effective *O*-mannosylation. Although several of the peptides shown in Fig. 1*B* have a PT motif, some of them did not work as an acceptor at all and others worked poorly as acceptors (Figs. 1*B* and 2, and Table 1). These results suggest that the preferential common sequence for effective *O*-mannosylation is present in peptides 336–355 and 401–420. Indeed, the presence of a Thr residue that is preferentially mannosylated was confirmed by MALDI-TOF MS analysis and amino acid sequence analysis of mannosylated peptides. We obtained mono-, di-, and tri-mannosyl peptides from peptide 401–420. Analysis of these products showed that a mono-mannosylated peptide was mannosylated mainly at Thr-414 and a di-mannosylated peptide was mannosylated at Thr-406 and Thr-414, and Thr-404 is the last of the Thr residues to be *O*-mannosylated. These results indicate that *O*-mannosylation of the Thr residues is highly ordered. Furthermore, peptide 401–420(T414Man) was a more effective acceptor than peptide 401–420, indicating that the mannosylation of Thr-414 leads to effective subsequent *O*-mannosylation. Therefore, α-DG appears to be a prominent acceptor of *O*-mannosylation because it has both the PT motif and the preferential sequences.

O-GalNAc glycosylation is the most common protein modification and is initiated by the action of a family of pp-GalNAc-Ts. Rules are thought to exist that specify which Ser and Thr residues become decorated with *O*-GalNAc. However, despite intense investigation, no consensus sequence has emerged that is both necessary and sufficient for *O*-GalNAc glycosylation to occur. Many nuclear and cytosolic proteins are *O*-GlcNAc glycosylated at a variety of attachment sites, but a consensus sequence for *O*-GlcNAc transferase has not been reported (20, 21). On the other hand, *O*-Fuc glycosylation exists in direct *O*-linkage to Ser or Thr residues in two different types of Cys knot motifs, epidermal growth factor-like repeats and thrombospondin type 1 repeats. The enzyme responsible for adding *O*-Fuc to epidermal growth factor repeats was identified as protein *O*-fucosyltransferase 1 (POFUT1), and the enzyme for adding to thrombospondin type 1 repeats was identified as POFUT2 (22, 23). A consensus sequence for *O*-Fuc glycosylation in epidermal growth factor is proposed,

$Cys X_{4-5}$(Ser/Thr)Cys between the second and third Cys residues, and a consensus sequence for *O*-Fuc in thrombospondin type 1 repeats is $Trp X_5 Cys X_{2/3}$Ser/Thr$Cys X_2 G$ between the first and second Cys residues, respectively (24–26). Both POFUT1 and POFUT2 require a specific sequence for *O*-Fuc glycosylation. Our results indicate that α-DG has preferred sequences for *O*-mannosylation. However, it may be that the efficiency of *O*-mannosylation depends not only on the sequence but also the secondary and tertiary structures.

Protein *O*-mannosylation is an essential post-translational modification (5). In yeast and fungi, protein *O*-mannosylation is indispensable for cell wall integrity and normal cellular morphogenesis (11). Protein *O*-mannosylation has also been suggested to be involved in the endoplasmic reticulum quality control system. In yeast, protein *O*-mannosylation is necessary for intracellular protein trafficking (11, 27). For example, it was found that nonnative proteins are *O*-mannosylated in the endoplasmic reticulum, which causes them to be excreted from the cell without aggregation and accumulation of aberrant proteins in the endoplasmic reticulum (28, 29). These results suggest that *O*-mannosyltransferases can recognize proteins that have undergone a conformational change. Thus, the conformation of a protein is another factor for *O*-mannosylation.

O-Mannosylation is an uncommon type of protein modification in mammals, but it is important in muscle and brain development (5). Although highly glycosylated α-DG was found to be selectively deficient in the skeletal muscle of WWS (7, 8), little is known about the molecular pathomechanism of WWS. Our results show that two peptides derived from the mucin domain of α-DG are highly *O*-mannosylated by POMT but that little or no *O*-mannosylation occurs in mucin tandem repeat peptides, suggesting that α-DG has multiple *O*-mannosylated glycans but other proteins have little, if any. The binding of ligands to glycans is known to depend on how the glycans are clustered. Binding of extracellular matrixes such as laminin, neurexin, and agrin may require a cluster of *O*-mannosyl glycan on α-DG. Therefore, a defect of *O*-mannosyl glycans in patients with WWS may severely affect α-DG functions but not other protein functions. Future studies may reveal how α-DG glycosylation contributes to muscular dystrophy and neuronal migration disorder and how normal glycosylation can restore functions of DG. Such studies may lead to the development of therapies for incomplete glycosylation-induced dystroglycanopathies.

Acknowledgment—We thank Fumihiko Ito for assistance in synthesizing mannosyl-threonine.

REFERENCES

1. Endo, T. (1999) *Biochim. Biophys. Acta* **1473,** 237–246
2. Chiba, A., Matsumura, K., Yamada, H., Inazu, T., Shimizu, T., Kusunoki, S., Kanazawa, I., Kobata, A., and Endo, T. (1997) *J. Biol. Chem.* **272,** 2156–2162
3. Michele, D. E., and Campbell, K. P. (2003) *J. Biol. Chem.* **278,** 15457–15460
4. Yoshida, A., Kobayashi, K., Manya, H., Taniguchi, K., Kano, H., Mizuno, M., Inazu, T., Mitsuhashi, H., Takahashi, S., Takeuchi, M., Herrmann, R., Straub, V., Talim, B., Voit, T., Topaloglu, H., Toda, T., and Endo, T. (2001) *Dev. Cell* **1,** 717–724
5. Endo, T. (2004) *Glycoconj. J.* **21,** 3–7
6. Manya, H., Chiba, A., Yoshida, A., Wang, X., Chiba, Y., Jigami, Y., Margolis, R. U., and Endo, T. (2004) *Proc. Natl. Acad. Sci. U. S. A.* **101,** 500–505
7. Beltran-Valero De Bernabe, D., Currier, S., Steinbrecher, A., Celli, J., Van Beusekom, E., Van Der Zwaag, B., Kayserili, H., Merlini, L., Chitayat, D., Dobyns, W. B., Cormand, B., Lehesjoki, A. E., Cruces, J., Voit, T., Walsh, C. A., Van Bokhoven, H., and Brunner, H. G. (2002) *Am. J. Hum. Genet.* **71,** 1033–1043
8. van Reeuwijk, J., Janssen, M., van den Elzen, C., Beltran-Valero de Bernabe, D., Sabatelli, P., Merlini, L., Boon, M., Scheffer, H., Brockington, M., Muntoni, F., Huynen, M. A., Verrips, A., Walsh, C. A., Barth, P. G., Brunner, H. G., and van Bokhoven, H. (2005) *J. Med. Genet.* **42,** 907–912
9. Akasaka-Manya, K., Manya, H., and Endo, T. (2004) *Biochem. Biophys. Res. Commun.* **325,** 75–79
10. Akasaka-Manya, K., Manya, H., Nakajima, A., Kawakita, M., and Endo, T. (2006) *J. Biol. Chem.* **281,** 19339–19345
11. Strahl-Bolsinger, S., Gentzsch, M., and Tanner, W. (1999) *Biochim. Biophys. Acta* **1426,** 297–307
12. Gentzsch, M., and Tanner, W. (1997) *Glycobiology* **7,** 481–486
13. Lehle, L., Strahl, S., and Tanner, W. (2006) *Angew. Chem. Int. Ed. Engl.* **45,** 6802–6818
14. Brancaccio, A., Schulthess, T., Gesemann, M., and Engel, J. (1995) *FEBS Lett.* **368,** 139–142
15. Yamada, H., Chiba, A., Endo, T., Kobata, A., Anderson, L. V., Hori, H., Fukuta-Ohi, H., Kanazawa, I., Campbell, K. P., Shimizu, T., and Matsumura, K. (1996) *J. Neurochem.* **66,** 1518–1524
16. Brancaccio, A., Schulthess, T., Gesemann, M., and Engel, J. (1997) *Eur. J. Biochem.* **246,** 166–172
17. Kanagawa, M., Saito, F., Kunz, S., Yoshida-Moriguchi, T., Barresi, R., Kobayashi, Y. M., Muschler, J., Dumanski, J. P., Michele, D. E., Oldstone, M. B., and Campbell, K. P. (2004) *Cell* **117,** 953–964
18. Takahashi, S., Sasaki, T., Manya, H., Chiba, Y., Yoshida, A., Mizuno, M., Ishida, H., Ito, F., Inazu, T., Kotani, N., Takasaki, S., Takeuchi, M., and Endo, T. (2001) *Glycobiology* **11,** 37–45
19. Ten Hagen, K. G., Fritz, T. A., and Tabak, L. A. (2003) *Glycobiology* **13,** 1R–16R
20. Vosseller, K., Wells, L., and Hart, G. W. (2001) *Biochimie (Paris)* **83,** 575–581
21. Wells, L., Vosseller, K., and Hart, G. W. (2001) *Science* **291,** 2376–2378
22. Wang, Y., Shao, L., Shi, S., Harris, R. J., Spellman, M. W., Stanley, P., and Haltiwanger, R. S. (2001) *J. Biol. Chem.* **276,** 40338–40345
23. Luo, Y., Koles, K., Vorndam, W., Haltiwanger, R. S., and Panin, V. M. (2006) *J. Biol. Chem.* **281,** 9393–9399
24. Harris, R. J., and Spellman, M. W. (1993) *Glycobiology* **3,** 219–224
25. Hofsteenge, J., Huwiler, K. G., Macek, B., Hess, D., Lawler, J., Mosher, D. F., and Peter-Katalinic, J. (2001) *J. Biol. Chem.* **276,** 6485–6498
26. Gonzalez de Peredo, A., Klein, D., Macek, B., Hess, D., Peter-Katalinic, J., and Hofsteenge, J. (2002) *Mol. Cell. Proteomics* **1,** 11–18
27. Proszynski, T. J., Simons, K., and Bagnat, M. (2004) *Mol. Biol. Cell* **15,** 1533–1543
28. Harty, C., Strahl, S., and Romisch, K. (2001) *Mol. Biol. Cell* **12,** 1093–1101
29. Nakatsukasa, K., Okada, S., Umebayashi, K., Fukuda, R., Nishikawa, S., and Endo, T. (2004) *J. Biol. Chem.* **279,** 49762–49772

FIGURE 5. MALDI-TOF MS and MS/MS spectra of mannosyl peptides. **(A),** MS spectrum of Con A-purified mannosyl peptides. Due to oxidation of the methionyl residue, +16Da peaks were detected (*m/z* 2289.2, 2451.2 and 2613.3). (B), MS/MS spectra of non-, mono-, di- and tri-mannosylated peptides. The calculated average mass value of b12 fragment ion is 1359.6. Each observed mass = *m/z*[b12]1360.2 (non-mannosyl spectrum), 1361.1 (mono-mannosyl spectrum), *m/z*[b12+Man]1522.6 (di-mannosyl spectrum), *m/z*[b12+2Man]1684.5 (tri-mannosyl spectrum).

SUPPLEMENTAL DATA

SUPPLEMENTARY FIGURE 1. Kinetics analysis of POMT activity against various peptides. Michaelis-Menten plots (A) and Hanes-Woolf plots (B) were based on the POMT reactions performed using various substrate concentrations: 0.25-4 mM of the acceptor peptide. s, concentration of acceptor peptide (mM); v, specific activity (pmol/h/mg total protein).

SUPPLEMENTARY FIGURE 2. Purification of mannosylated peptide 401-420 by sequential Con-A Sepharose column followed by reversed-phase HPLC. POMT reaction was performed in a 30 μl reaction volume containing 20 mM Tris-HCl (pH 8.0), 300 μM Dol-P-Man, 2 mM dithiothreitol, 10 mM EDTA, 0.5% *n*-octyl-β-D-thioglucoside, 1 mM peptide 401-420 and 120 μg of microsomal membrane fraction at 25°C for 2h. The panels show reversed-phase HPLC (Wakopak 5C18-200 column) chromatograms of the reaction mixture (A), the fraction of the reaction mixture that did not bind to a Con A-Sepharose column (B) and the fraction of the reaction mixture that bound to the Con A-Sepharose column (C). The closed triangles indicate the original peptide 401-420 and the open triangles indicate the mannosylated products. Dashed line shows acetonitrile concentration.

SUPPLEMENTARY FIGURE 3. Subtracted chromatograms of mannosyl peptide by Edman degradation. Mono-, di- and tri-mannosylated peptides were subjected to amino acid sequencing. The chromatograms of 4th, 6th, 14th or 18th cycles in Edman degradation were subtracted from those of the previous cycles. PTH-Thr (T) was eluted at 6 min, and mannosyl-Thr-related peaks (T-M) were eluted at 4.4 and 5.5 min. The retention times of these peaks were identical to those of peaks analyzed synthetic mannosyl threonine. The mono-mannosylated peptide was mannosylated mainly at Thr414, the di-mannosylated peptide was mannosylated at Thr406 and Thr414, and the tri-mannosylated peptide was mannosylated at Thr404, Thr406, and Thr 414.

SUPPLEMENTARY FIGURE 4. Sequential *O*-mannosylation of the peptide 401-420. POMT reaction was performed for 15-120 min under the condition as mentioned in supplemental Fig. 2. The panels show reversed-phase HPLC (Mightysil RP-18GP Aqua column) chromatograms of the fraction of the reaction mixture that bound to the Con A-Sepharose column. The arrowheads indicate the migration positions of (I) mono-, (II) di- and (III) tri-mannosylated peptides.

SUPPLEMENTARY FIGURE 5. Effect of Thr414-mannosylation on POMT activity. (A), Amino acid sequence of mono-mannosylpeptide 401-420(T414Man). Michaelis-Menten plots (B) and Hanes-Woolf plots (C) were based on the POMT reactions performed using various substrate concentrations: 0.025-1 mM of the acceptor peptide. s, concentration of acceptor peptide (mM); v, specific activity (pmol/h/mg total protein).

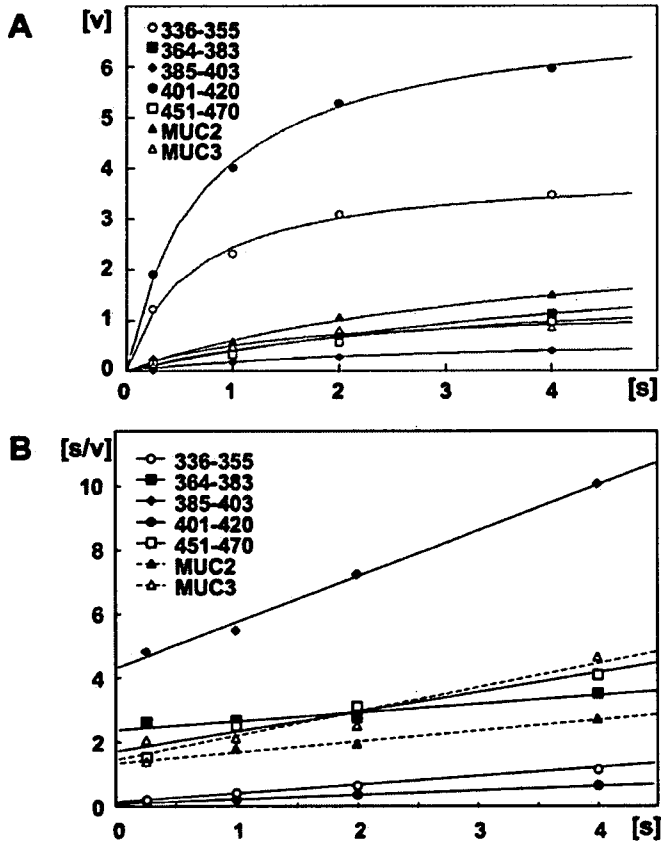

Supplementary Figure 1, Manya et al.

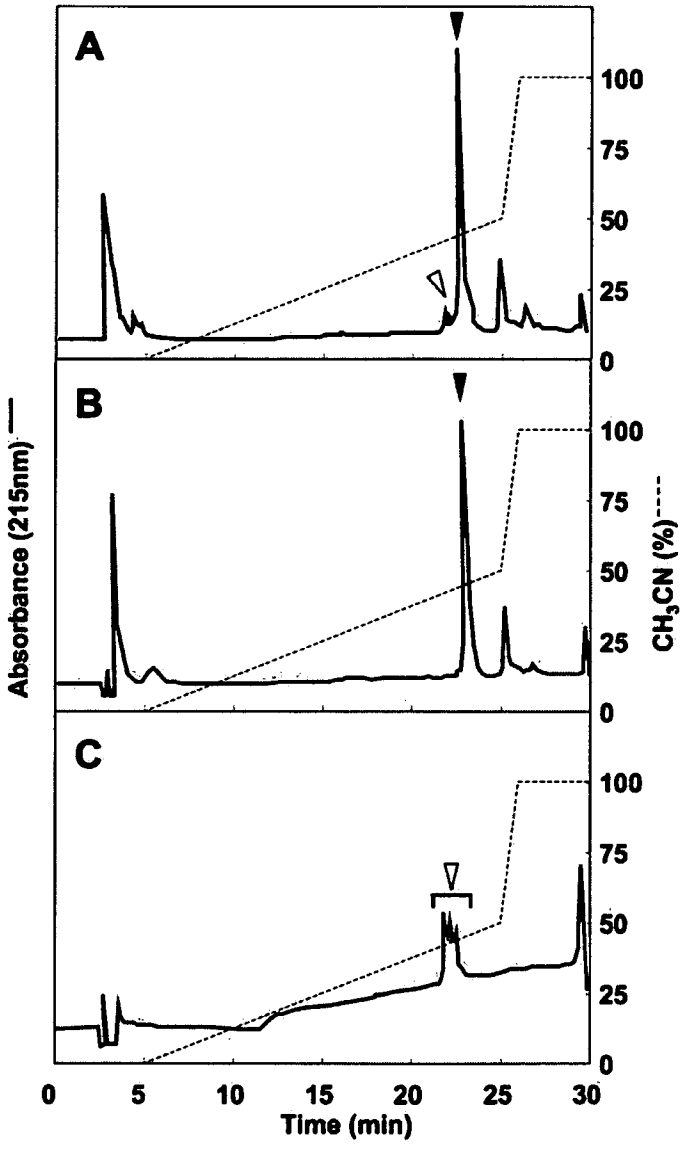

Supplementary Figure 2, Manya et al.

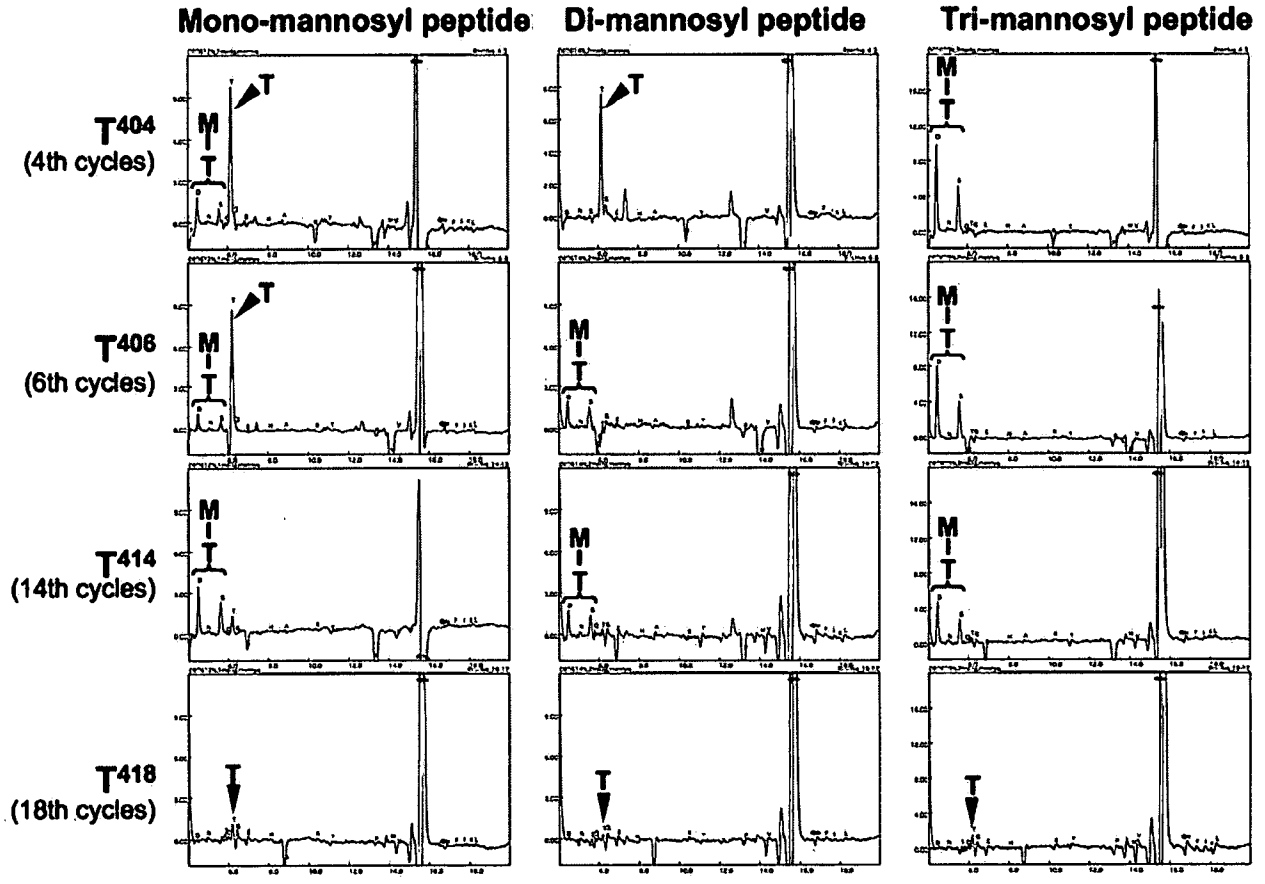

Supplementary Figure 3, Manya et al.

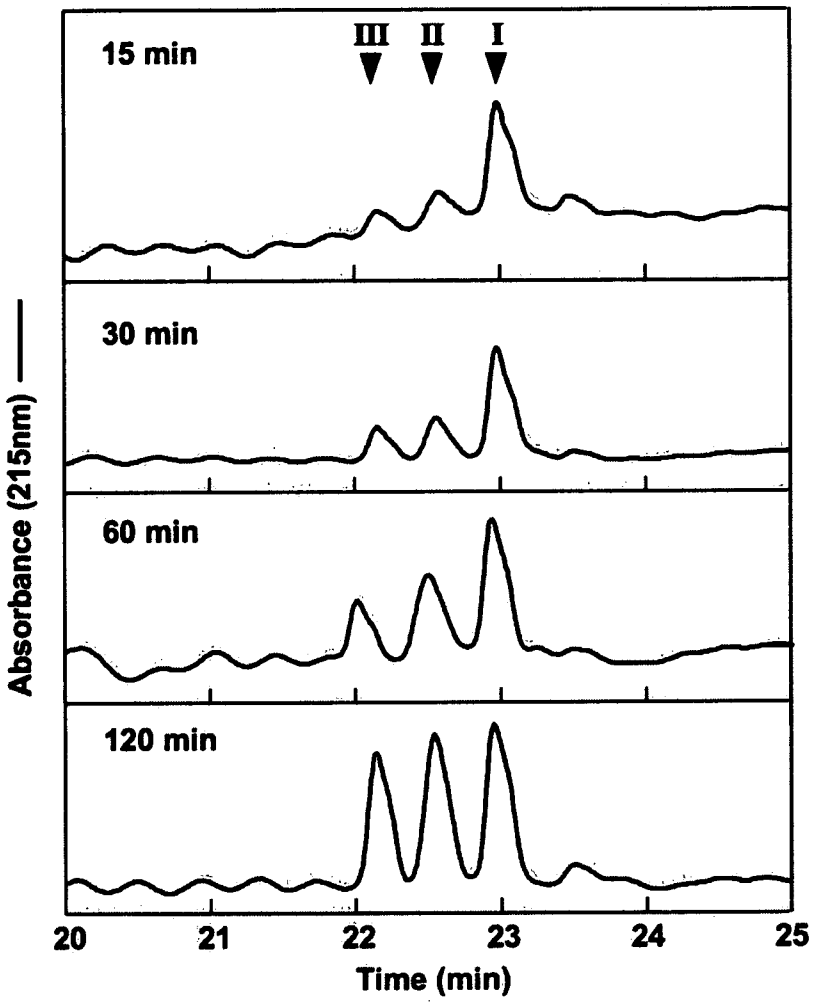

Supplementary Figure 4, Manya et al.

A IRPTMTIPGYVEPT (Man) AVATPP

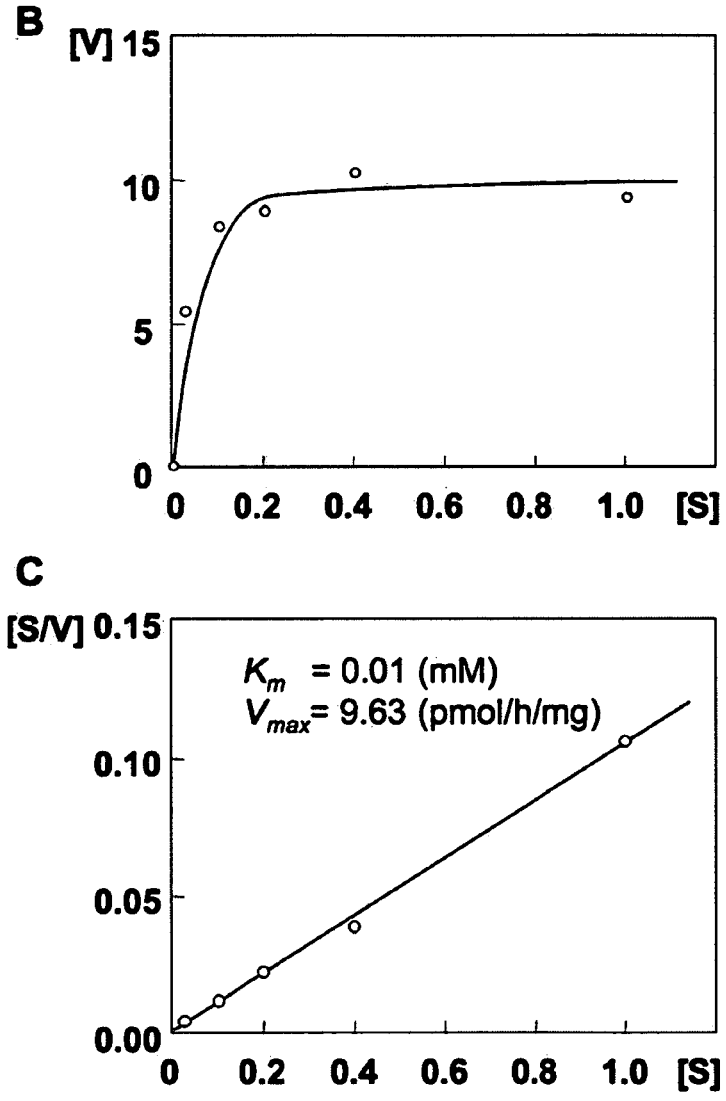

Supplementary Figure 5, Manya et al.

ELSEVIER

Neuromuscular Disorders 18 (2008) 45–51

www.elsevier.com/locate/nmd

Protein *O*-mannosyltransferase activities in lymphoblasts from patients with α-dystroglycanopathies

Hiroshi Manya [a,1], Céline Bouchet [b,1], Akiko Yanagisawa [c,d], Sandrine Vuillaumier-Barrot [b], Susana Quijano-Roy [c,d,e], Yasushi Suzuki [f], Svetlana Maugenre [c,d], Pascale Richard [c,d,g,h], Toshiyuki Inazu [f,i], Luciano Merlini [j], Norma B. Romero [c,d], France Leturcq [k], Isabelle Bezier [l], Haluk Topaloglu [m], Brigitte Estournet [e], Nathalie Seta [b,*], Tamao Endo [a], Pascale Guicheney [c,d,h]

[a] *Glycobiology Research Group, Tokyo Metropolitan Institute of Gerontology, Foundation for Research on Aging and Promotion of Human Welfare, Itabashi-ku, Tokyo, Japan*
[b] *AP-HP, Bichat-Claude Bernard Hospital, Biochimie, INSERM CRB U773, Paris, France*
[c] *Inserm, U582, Institut de Myologie, Paris, France*
[d] *Université Pierre et Marie Curie-Paris6, UMR S582, IFR14, Paris, France*
[e] *AP-HP, Raymond Poincaré Hospital, Pédiatrie, Garches, France*
[f] *Department of Applied Chemistry, School of Engineering, Tokai University, Kanagawa, Japan*
[g] *AP-HP, Pitié-Salpêtrière Hospital, UF Cardiogénétique et Myogénétique, Paris, France*
[h] *AP-HP, Pitié-Salpêtrière Hospital, Service de Biochimie B, Paris, France*
[i] *Institute of Glycotechnology, Tokai University, Kanagawa, Japan*
[j] *Dipartimento di Medicina Sperimentale e Diagnostica, Sezione di Genetica Medica, Muscle Unit, Università di Ferrara, Italy*
[k] *AP-HP, Cochin Hospital, Biochimie et Génétique Moléculaire, 75014 Paris, France*
[l] *Banque de Cellules et d'ADN Genethon, Evry, France*
[m] *Department of Pediatric Neurology, Hacettepe University, Ankara, Turkey*

Received 11 May 2007; received in revised form 23 July 2007; accepted 8 August 2007

Abstract

Defects in *O*-mannosylation of α-dystroglycan cause some forms of congenital muscular dystrophy (CMD), the so-called α-dystroglycanopathies. Six genes are responsible for these diseases with overlapping phenotypes.

We investigated the usefulness of a biochemical approach for the diagnosis and investigation of the α-dystroglycanopathies using immortalized lymphoblasts prepared from genetically diagnosed and undiagnosed CMD patients and from control subjects. We measured the activities of protein *O*-mannose β1,2-*N*-acetylglucosaminyltransferase 1 (POMGnT1) and protein *O*-mannosyltransferase (POMT). Lymphoblasts from patients harbouring known mutations in either *POMGNT1* or *POMT1* showed a marked decrease in POMGnT1 or POMT activity, respectively, compared to controls. Furthermore, we identified pathogenic mutations in *POMGNT1*, *POMT1* or *POMT2* in six previously genetically uncharacterised patients who had very low enzyme activity. In conclusion, the lymphoblast-based enzymatic assay is a sensitive and useful method (i) to select patients harbouring *POMGNT1*, *POMT1* or *POMT2* mutations; (ii) to assess the pathogenicity of new or already described mutations.

Keywords: POMT1; POMT2; POMGnT1; Congenital muscular dystrophy; Enzyme activity

1. Introduction

α-Dystroglycan (α-DG) is a heavy glycosylated membrane protein, and its glycan groups have been shown

* Corresponding author. Tel.: +33 1 40 25 85 43; fax: +331 40 25 88 21.
E-mail address: nathalie.seta@bch.aphp.fr (N. Seta).
[1] The authors wish it to be known that, in their opinion, the first two authors should be regarded as joint First Authors.

0960-8966/$ - see front matter © 2007 Elsevier B.V. All rights reserved.
doi:10.1016/j.nmd.2007.08.002

to play a major role in binding to extracellular matrix proteins such as laminin, neurexin, and agrin [1,2]. In humans, defects in the *O*-glycosylation of α-DG cause a large spectrum of autosomal recessive congenital muscular dystrophies (CMD), from mild forms without central nervous system (CNS) involvement to more severe forms with structural brain and eye abnormalities such as muscle–eye–brain disease (MEB: OMIM 253280) and Walker–Warburg syndrome (WWS: OMIM 236670). These entities are now collectively classified as the α-dystroglycanopathies [3].

Mutations in *POMGNT1* were first identified in patients with MEB [4,5] and soon after mutations in *POMT1* [6–9] and *POMT2* [10] were reported in children affected with WWS. In fact, the clinical spectrum associated with these three genes is broad and extends from patients with severe mental retardation and limited life expectancy to being able to walk and survive into the second decade of life.

In addition to MEB and WWS, other muscular dystrophies have been reported to be associated with an abnormal glycosylation of α-DG: Fukuyama-type congenital muscular dystrophy (FCMD: OMIM 253800), CMD type 1C (MDC1C: OMIM 606612), limb–girdle muscular dystrophy type 2I (LGMD2I: OMIM 607155), and CMD type 1D (MDC1D: OMIM 608840). FCMD, due to mutations in *fukutin*, has been reported almost exclusively in patients of Japanese origin who present with a CMD associated with mental retardation, brain malformations with or without eye involvement [11]. Regarding MDC1D, two cases with *LARGE* mutations have been reported in the literature, in a mentally retarded girl with brain abnormalities [12] and a family with WWS [13]. In contrast, *FKRP* mutations are responsible for the most common form of α-dystroglycanopathy in Western countries, a relatively mild disease that presents with limb–girdle weakness in childhood or adulthood and normal intelligence (LGMD2I). Less commonly, mutations in *FKRP* have been reported in patients with mental retardation, transitory brain white matter abnormalities and brain stem and *posterior fossa* malformations (MDC1C) [14–17] and even in patients with MEB and WWS, showing the overlap in phenotypes that is possible among the α-dystroglycanopathies [18]. As a further example of this overlap, *POMGNT1*, *POMT1* and *POMT2* mutations have been recently identified in patients with much milder phenotypes than the initial descriptions of a typical MEB or WWS [17,19–23]. Since multiple genes are known to cause α-dystroglycanopathies, with an extremely broad clinical spectrum and relatively poor phenotype–genotype correlation, at present molecular diagnosis of α-dystroglycanopathy patients is difficult and requires searching for mutations gene by gene.

With the aim of improving the diagnosis and investigation of patients with an α-dystroglycanopathy, we investigated the utility of a biochemical approach. At present, of the six known α-dystroglycanopathy genes, the function of the protein product is clear only for POMT1 and POMT2, which are responsible for the catalysis of the first step in *O*-mannosyl glycan synthesis [24] and POMGnT1 which forms a GlcNAcβ1–2 Man linkage of *O*-mannosyl glycans on α-DG [4]. An assay for POMGnT1 activity in lymphoblasts has previously been described [25]. In previous studies, we demonstrated by a specific enzymatic activity assay that mutations in *POMGNT1* and *POMT1* lead to defects in POMGnT1 and POMT activity, respectively, using mutant constructs transfected into cell lines [24,26]. In order to screen patients with confirmed or suspected forms of α-dystroglycanopathy, we developed an assay for lymphoblast POMT activity and measured the activities of both POMT and POMGnT1 in lymphoblasts from a series of patients. We observed reductions in POMGnT1 or POMT activity in several uncharacterised patients, in whom secondary targeted sequencing led to the identification of mutations in *POMT1*, *POMT2* or *POMGNT1*.

2. Experimental procedures

2.1. Patients

Blood from seven healthy subjects and 24 CMD patients with high serum creatine kinase levels, and with or without mental retardation was collected for B lymphoblast immortalization and DNA extraction after informed consent. Eleven patients had already been genetically characterised. Seven patients had mutations in *FKRP*, two in *POMGNT1* [4] and two in *POMT1* [21,22] (**Table 1**). Thirteen other patients were genetically uncharacterised (GUC1–GUC13) before the enzymatic studies. These 13 patients were all CMD patients with or without mental retardation, brain abnormality and ocular involvement, and in five of them, marked hypoglycosylation of α-DG was observed by immunohistochemistry or Western blot analysis in muscle biopsies. The α-DG status in the eight other cases could not be evaluated, because no muscle was available. *FKRP* had been sequenced and excluded in all of these 13 cases prior to the enzymatic studies. Afterwards *LARGE* and *fukutin*, and then *POMT1*, *POMT2* and *POMGNT1* were sequenced in the patients for whom no decrease in the enzymatic activities was found.

2.2. Cell culture and extract preparation

B lymphoblastoid cell lines were obtained after immortalization by Epstein–Barr virus and cultured in RPMI 1640 (Invitrogen, Carlsbad, CA) according to standard protocols to obtain 100×10^6 cells. After centrifugation at 800*g* for 5 min, the pellets were rinsed twice with 50 ml then with 12 ml of phosphate-buffered saline (PBS). The final pellets were frozen at −80 °C. The cells ($\sim 7.5 \times 10^6$ cells) were homogenized in 10 mM Tris–HCl, pH 7.4, 1 mM EDTA, 250 mM sucrose, 1 mM dithiothreitol, with a protease inhibitor cocktail (3 μg/ml pepstatin A, 1 μg/ml leupeptin, 1 mM benzamidine–HCl, and 1 mM PMSF). After centrifugation at 900*g* for 10 min, the supernatant was subjected to ultra centrifugation at

Table 1
POMGNT1, *POMT1* and *POMT2* mutations evidenced in patients with low POMGnT1 or POMT activities

Patient	Gene	Allele 1	Allele 2	References
GC8	*POMT1*	p.Gly65Arg	p.Trp582Cys	[21]
GC9	*POMT1*	p.Ala200Pro	p.Ala200Pro	[20]
GC10	*POMGNT1*	c.1539+1 G>A	c.1539+1 G>A	[4]
GC11	*POMGNT1*	p.Arg442His	p.Arg442His	Unpublished
GUC1	*POMGNT1*	p.Ser153X	p.Cys269del	Unpublished
GUC2	*POMT1*	p.Ala669Thr	p.Gly722fs>730x	Unpublished
GUC3	*POMT2*	p.Tyr96Cys	p.Tyr96Cys	Unpublished
GUC4	*POMT2*	p.Tyr666Cys	p.Tyr666Cys	[22]
GUC5	*POMT2*	p.Tyr666Cys	Splicing abnormality	Unpublished
GUC6	*POMT2*	p.Tyr666Cys	p.Trp748Arg	[22]

(GC: genetically characterised patient, GUC: genetically uncharacterised patient).

100,000*g* for 1 h. The precipitate was used as the microsomal membrane fraction. Protein concentrations were determined by the BCA assay (PIERCE, Rockford, IL). About 40 μg of protein was obtained in the microsomal membrane fraction prepared from 1×10^6 cells.

2.3. Assay for POMGnT1 activity

POMGnT1 activity was obtained from the amount of [^{3}H]GlcNAc transferred to a mannosylpeptide [4,25]. The reaction buffer containing 140 mM MES buffer (pH 7.0), 1 mM UDP-[^{3}H]GlcNAc (225,000 dpm/nmol) (Perkin-Elmer, Inc., Waltham, MA), 1 mM mannosyl nanopeptide (Ac-Ala-Ala-Pro-Thr(Man)-Pro-Val-Ala-Ala-Pro-NH_2), 10 mM $MnCl_2$, 2% Triton X-100, 5 mM AMP, 200 mM GlcNAc, 10% glycerol and enzyme source (100 μg of microsomal membrane fraction) in 20 μl total volume was incubated at 37 °C for 4 h. After boiling for 3 min, the mixture was analyzed by reversed phase HPLC with a Wakopak 5C18–200 column (4.6 × 250 mm, Wako Pure Chemical Industries, Ltd., Osaka, Japan). Solvent A was 0.1% trifluoroacetic acid in distilled water and solvent B was 0.1% trifluoroacetic acid in acetonitrile. The peptide was eluted at a flow rate of 1 ml/min using a linear gradient of 1–25% solvent B. The peptide separation was monitored continuously at 214 nm, and the radioactivity of each fraction was measured using a liquid scintillation counter.

2.4. Assay for POMT activity

The POMT activity was based on the amount of [^{3}H]-mannose transferred to a glutathione-*S*-transferase fusion α-DG (GST-αDG) as described previously [27]. Briefly, the reaction mixture contained 20 mM Tris–HCl (pH 8.0), 100 nM of [^{3}H]-mannosylphosphoryldolichol (Dol-P-Man, 125,000 dpm/pmol) (American Radiolabeled Chemical, Inc., St. Louis, MO), 2 mM 2-mercaptoethanol, 10 mM EDTA, 0.5% *n*-octyl-β-D-thioglucoside, 10 μg GST-α-DG and enzyme source (80 μg of microsomal membrane fraction) in 20 μl total volume. After 1 h incubation at 22 °C, the reaction was stopped by adding 150 μl PBS containing 1% Triton X-100, and the reaction mixture was centrifuged at 10,000*g* for 10 min. The supernatant was removed, mixed with 400 μl of PBS containing 1% Triton X-100 and 10 μl of Glutathione–Sepharose 4B beads (GE Healthcare Bio-Sciences Corp., NJ, USA), rotated at 4 °C for 1 h, and washed three times with 20 mM Tris–HCl (pH 7.4) containing 0.5% Triton X-100. The radioactivity adsorbed to the beads was measured using a liquid scintillation counter.

2.5. Assay for GnT1 activity

The GnT1 (UDP–GlcNAc: α-3-D-mannoside β1,2-*N*-acetylglucosaminyltransferase 1, EC 2.4.1.101) activity was performed in a total volume of 20 μl reaction mixture containing 100 mM MES buffer, 10 μM pyridylaminated $Man_5GlcNAc_2$ (M5-PA, Takara Bio Inc., Otsu, Japan), 2 mM UDP–GlcNAc, 5 mM AMP, 0.5% Triton X-100, 0.2% BSA, 20 mM $MnCl_2$ and enzyme source (100 μg of microsomal membrane fraction) at 37 °C for 2 h. The samples were then analyzed by reversed phase HPLC with a COSMOSIL 5C18-AR-II column (4.6 × 250 mm, Nacalai Tesque, Kyoto, Japan). The solvent used was a 100 mM, pH 6.0, ammonium acetate buffer containing 0.15% 1-butanol, and the substrate and the product were isocratically separated. Fluorescence was detected with a fluorescence detector (RF-10AXL, Shimadzu Corp., Kyoto, Japan) at excitation and emission wavelengths of 320 nm and 400 nm, respectively.

2.6. Mutation analysis

Genomic DNA was extracted from lymphoblasts using standard methods. Primer pairs were designed to amplify all coding exons and flanking intronic sequences of *POMT1* (9q34.1), *POMT2* (14q24) and *POMGNT1* (1p34.1). The primer sequences and PCR conditions are available upon request. The generated amplicons were purified and directly sequenced with the BigDye terminator kit (Perkin-Elmer Applied Biosystems, Wellesley, MA). Sequences were analyzed on an ABI PRISM 31130 capillary sequencer (Applera, CA). One hundred unrelated healthy individuals served as control subjects to test the presence of the missense mutations p.Tyr96Cys and p.Tyr666Cys (*POMT2*), and p.Ala669Thr (*POMT1*) by sequencing.

3. Results

3.1. GnT1 activity

GnT1 present in the Golgi apparatus is the entry point for the conversion of oligomannose to hybrid and complex *N*-glycans. Since GnT1 is not involved in *O*-mannosylglycan biosynthesis, it is not affected in α-dystroglycanopathies and represents a suitable control to normalise samples for baseline microsomal activity. The high consistent levels of cellular GnT1 activity as shown in Fig. 1, gives an indication of the quality of the cells we used for enzyme analysis. The GnT1 activity mean (±standard deviation) of all samples was 0.53 (±0.06) nmol/h/mg total proteins.

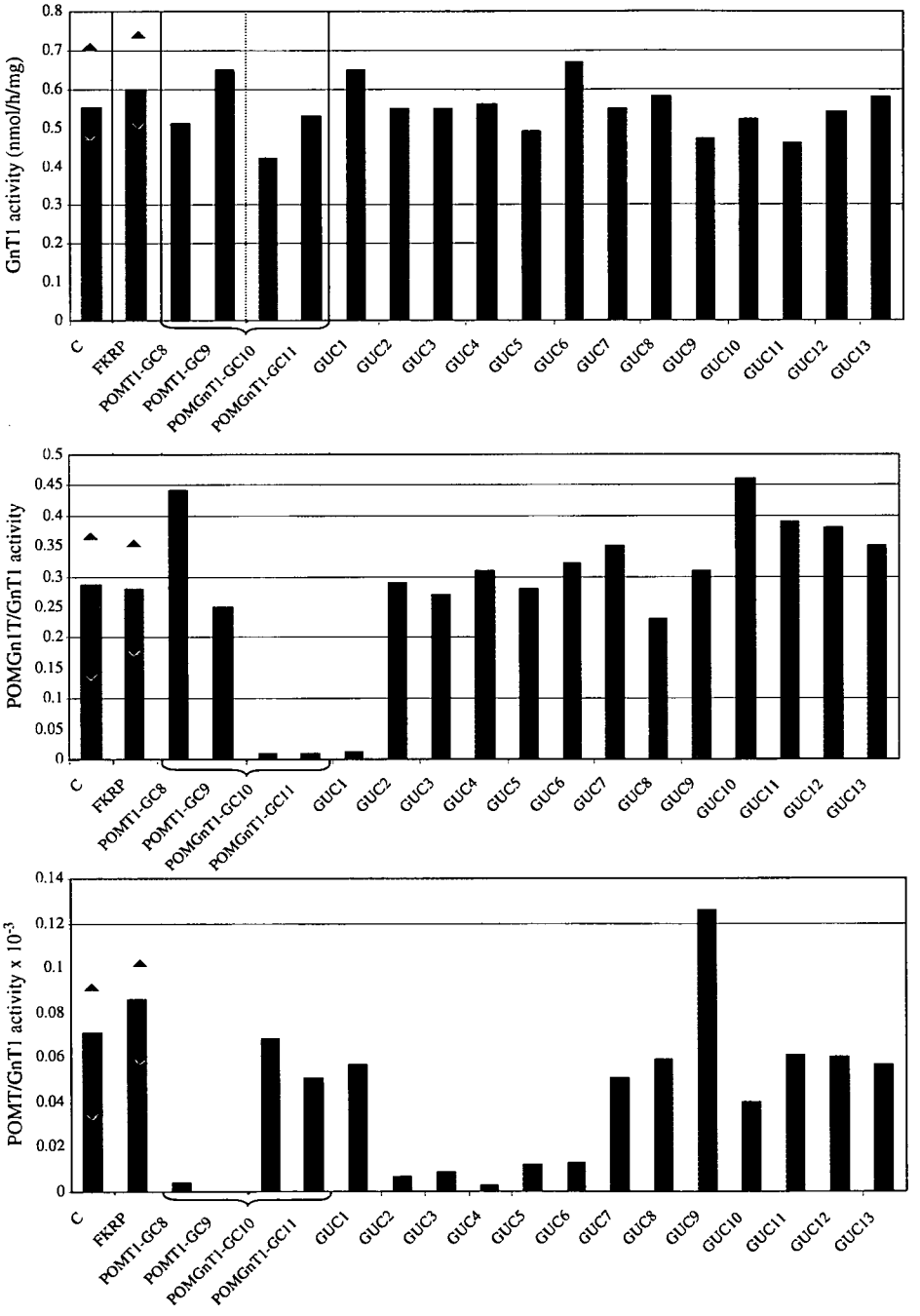

Fig. 1. Lymphoblast GnT1, POMGnT1/GnT1 and POMT/GnT1 activities from controls and patients with FKRP mutations, and patients with congenital muscular dystrophy: genetically characterised patients (GC8–GC11) and uncharacterised patients (GUC1–GUC13). For Controls (C) and FKRP-patients (FKRP) mean [minor–major value].

3.2. POMGnT1 activity

The average POMGnT1 activity measured in lymphoblasts of control subjects was 0.163 (±0.042) nmol/h/mg total proteins. When we assessed the POMGnT1 activity of patient lymphoblasts, we observed a decrease for three of them. Two had previously been genetically confirmed with mutations in *POMGNT1* (Table 1). Patient GC10 carried the common MEB mutation, c.1539 + 1G > A in the homozygous state, and patient GC11 harboured the mutation p.Arg442His, also in homozygous state. POMGnT1 activity in these lymphoblasts was much lower (0.005 and 0.006 nmol/h/mg total protein, respectively.) than in the control subjects and the other patients.

Among all the other patients, only one patient, GUC1, showed low POMGnT1 activity (0.008 nmol/h/mg), similar to GC10 and GC11, and was thus secondarily screened for *POMGNT1*. The DNA study of this patient revealed two heterozygous mutations: a nonsense mutation, p.Ser153X (c.458C > G), which probably leads to a loss of function, and a deletion of three base pairs c.805–807delTGC, which is expected to delete one amino acid, cysteine at position 269 (p.Cys269del). A missense mutation, p.Cys269Tyr, affecting the same amino acid has already been reported [28], and *in vitro* enzymatic activity was undetectable in the mutant protein carrying this substitution [24]. Thus, the 269 cysteine deletion is very likely to be pathogenic. DNA study confirmed the heterozygous carrier status of both parents.

The ratios of POMGnT1 activity to GnT1 activity were on average 0.01 in patients with POMGNT1 mutations ($n = 3$), and 0.29 in controls ($n = 7$) (Fig. 1). The presence of different FKRP mutations did not affect lymphoblast POMGnT1 activity in the seven patients, as shown by POMGnT1/GnT1 activity ratio, which was similar to that of controls (0.28).

3.3. POMT activity

Using the same controls as for POMGnT1, we assayed the POMT activity for the first time in lymphoblasts of control subjects and found the average value was 0.041 (±0.013) pmol/h/mg proteins. It is notable that the POMT activity in these cells was much lower than the POMGnT1 activity.

When we assessed POMT activity in the 17 patient lymphoblasts without *FKRP* mutations, we observed markedly reduced activity in seven of them (GC8 and 9, GUC2, 3, 4, 5 and 6) (Fig. 1). Two had been previously genetically confirmed with mutations in the *POMT1*. Patient GC9 was homozygous for the missense mutation p.Ala200Pro [21], and patient GC8 was a compound heterozygous carrier of two missense mutations, p.Gly65Arg and p.Trp582Cys [22]. The enzyme activity in these patient lymphoblasts was extremely low: undetectable in patient GC9 and 0.002 pmol/h/mg proteins in patient GC8. These last results strongly support the pathogenicity of the previously identified mutations.

The five other patients were secondarily screened for *POMT1* and *POMT2* (Table 1). We found two heterozygous mutations, in *POMT1* for patient GUC2: p.Ala669Thr (c.2005G > A), associated with c.2167insG which leads to a premature stop codon in amino acid 730. These mutations were already described [6,20]. POMT activity of this patient was 0.004 pmol/h/mg proteins. Targeted sequencing of patients GUC3, GUC4, GUC5 and GUC6, whose POMT activity was 0.005, 0.001, 0.006 and 0.009 pmol/h/mg proteins, respectively, showed *POMT2* mutations (Table 1). Patients GUC3 and GUC4 harboured missense mutations in the homozygous state, respectively, p.Tyr96Cys (c.287A > G) and p.Tyr666Cys (c.1997A > G). These missense mutations are situated in highly conserved regions. The p.Tyr666Cys recently described as a founder mutation [23], was found in the heterozygous state in patients GUC5 (maternal allele) and GUC6. In patient GUC6, the second mutation was a missense mutation, p.Trp748Arg (c.2242T > C). In addition, patient GUC5 had on the other (paternal) allele a four base pair deletion in exon 1, 46 base pairs before the initiating ATG (c.1–46_49del CAGA). This change was also found in 4.2% of control DNA samples, and therefore is very unlikely to be pathogenic. Further analysis of patient cDNA showed a *POMT2* transcript missing exons 3–5, which is predicted to lead to a premature stop codon (data not shown). This transcript was also found in cDNA generated from paternal lymphoblasts. The corresponding pathogenic mutation remains to be identified at the genomic level. Patient GUC3 carrying a homozygous *POMT2* missense mutation p.Tyr96Cys had a classical severe WWS phenotype and died at age 2.5 years. In contrast, patients carrying the p.Tyr666Cys mutation in the homozygous or heterozygous state were less severely affected, having CMD with mental retardation, but without severe brain abnormalities on MRI. The p.Tyr96Cys (c.287A > G) *POMT2* mutation has not been previously described. The screening of 200 alleles from healthy unrelated individuals did not reveal any of these mutations.

The ratios of POMT/GnT1 activity were on average 0.005×10^{-3} in patients with *POMT1* or *POMT2* mutations, and 0.071 $(\pm 0.019) \times 10^{-3}$ in controls, respectively (Fig. 1). As for POMGnT1 activity, the seven patients with *FKRP* mutations presented similar lymphoblast POMT activity, compared to control values, as confirmed by the POMT/GnT1 activity ($0.086 \pm 0.019 \times 10^{-3}$).

4. Discussion

The recent identification of six genes associated with the α-dystroglycanopathies has made it possible to establish a precise molecular diagnosis in many families, but since there is such an overlap in clinical features between genes, successive genes must be sequenced to identify the causative mutations in sporadic cases. These methods are expensive and time-consuming. To direct genetic analysis, firstly a POMGnT1 enzymatic assay was reported based

on extracts of muscle biopsies [29], and more recently fibroblast- and lymphoblast-based assays have been developed [25]. The average residual POMGnT1 activity in fibroblasts and lymphoblasts from MEB patients was about 13% and 15% of normal controls, and this fibroblast- and lymphoblast-based assay was proposed as a rapid and relatively simple diagnostic test for MEB patients [25].

In a similar manner, we have developed an assay to determine POMT activity in patient lymphoblasts. We had previously measured *in vitro* POMT activity in Sf9 cells transfected with various *POMT1* mutants [26]. We now show that POMT activity can be measured in control and patient lymphoblasts. As the previous descriptions [25,29], measuring GnT1 activity in parallel allows validation of the cell preparation and the POMT and POMGnT1 activity measurement quality. When testing cells from patients with known *POMT1* mutations, activity levels were almost undetectable. A marked reduction in POMT activity was also found in five genetically uncharacterised patients, which led us to sequence *POMT1* and *POMT2*. We identified mutations in all of these patients, and most of them are either previously reported or novel missense mutations that were absent from control chromosomes. As for POMGnT1 activity, the lymphoblast-based enzymatic POMT assay is inexpensive and precise, and may bypass the need for invasive muscle biopsies when clinical findings are highly suggestive of an α-dystroglycanopathy. These tests can also be used to assess the pathogenicity of the new mutations, as well as those already described, to ascertain their pathogenicity.

Patients GC9 and GC8 carrying *POMT1* missense mutations showed relatively mild phenotypes compared to typical WWS. The Turkish patient (GC9), homozygote for the p.Ala200Pro mutation, had LGMD2I with mild mental retardation and microcephaly [21], while the phenotype of the Italian patient (GC8), who is compound heterozygous for the p.Gly65Arg and p.Trp582Cys mutations, had CMD with calf muscle pseudohypertrophy, microcephaly and severe mental retardation, but no eye abnormalities, and was still living at the age of 19 years [22]. These phenotypic features had led us to expect that these mutations would not completely abolish POMT activity. However, these patients have very low or undetectable enzyme activities. At this stage, the discrepancy between clinical severity and the level of POMT activity of these patients remains unexplained.

To date, *POMT2* mutations have been reported in CMD patients with both a severe phenotype, WWS, and a milder phenotype with mental retardation [22,23,30]. The new homozygous missense *POMT2* mutation, p.Tyr96Cys, caused a typical WWS phenotype. In contrast the other three patients carrying p.Tyr666Cys were affected less severely [23].

In seven CMD patients, no decrease in POMT or POMGnT1 activity was observed. Two of these patients were confirmed to have marked hypoglycosylation of α-DG on muscle immunohistochemistry. To further investigate the basis of the CMD, we sequenced the coding exons and flanking intronic regions of all six genes known to cause α-dystroglycanopathy, without finding mutations. These results suggest that new genes involved in α-DG metabolism may be responsible for the disease in these patients.

Patients with *FKRP* mutations did not show reduced activity for POMT and POMGnT1 suggesting that FKRP is not associated with POMT1 or POMT2, or with POMGnT1. However, it has been recently reported that fukutin is associated with POMGnT1 in the Golgi compartment. Although fukutin has no proven glycosyltransferase activity, transgenic knock-in mouse carrying the retrotransposon insertion in the *fukutin* gene showed a 30% reduction of POMGnT1 activity [31], suggesting that fukutin modulates POMGnT1 activity in muscle. It will be interesting to test POMGnT1 activity in muscle, lymphoblasts and fibroblasts from FCMD patients to determine whether mutations in *fukutin* could modulate POMGnT1 activity.

Initially, muscle biopsies were used to test enzyme activity since α-DG, one of the only *O*-mannosylated glycoproteins identified up to now, is expressed in this tissue in addition to brain. This study shows that not only POMGnT1 but POMT1 and POMT2 are expressed in lymphoblasts also. Their precise role in lymphoblasts is not known, but α-DG was recently identified at both the mRNA and protein level in murine T and B lymphocytes [32]. It is also possible that additional proteins may also be *O*-mannosylated in human blood cells. In conclusion, our investigations show that the lymphoblast-based enzymatic assays are accurate and useful methods to select patients harbouring *POMT1*, *POMT2* and *POMGNT1* mutations among those with a suspected or confirmed α-dystroglycanopathy. In addition, they are robust functional tests that can be used to assess the pathogenicity of mutations.

Acknowledgements

We thank the patients and their families for their participation and Dr. Nigel Clarke for reviewing the manuscript. This work was supported by Research Grants for Nervous and Mental Disorders (17A-10) and Research on Psychiatric and Neurological Diseases and Mental Health from the Ministry of Health, Labour and Welfare of Japan, a Grant-in-Aid for Scientific Research on Priority Area (14082209) from the Ministry of Education, Culture, Sports, Science and Technology of Japan, the Institut National de la Santé et de la Recherche Médicale (INSERM), Association Française contre les Myopathies (AFM), the GIS-Institut des Maladies Rares (France) and EUROGLYCANET (Contract No. LSHM-CT2005-512131).

References

[1] Michele DE, Barresi R, Kanagawa M, et al. Post-translational disruption of dystroglycan–ligand interactions in congenital muscular dystrophies. Nature 2002;418:417–22.

[2] Michele DE, Campbell KP. Dystrophin–glycoprotein complex: post-translational processing and dystroglycan and function. J Biol Chem 2003;278:15457–60.
[3] Muntoni F, Voit T. 133rd ENMC International Workshop on Congenital Muscular Dystrophy (IXth International CMD Workshop) 21–23 January 2005, Naarden, The Netherlands. Neuromuscul Disord 2005;15:794–801.
[4] Yoshida A, Kobayashi K, Manya H, et al. Muscular dystrophy and neuronal migration disorder caused by mutations in a glycosyltransferase, POMGnT1. Dev Cell 2001;1:717–24.
[5] Diesen C, Saarinen A, Pihko H, et al. POMGnT1 mutation and phenotypic spectrum in muscle–eye–brain disease. J Med Genet 2004;41:e115.
[6] Beltran-Valero de Bernabe D, Currier S, Steinbrecher A, et al. Mutations in the *O*-mannosyltransferase gene POMT1 give rise to the severe neuronal migration disorder Walker–Warburg syndrome. Am J Hum Genet 2002;71:1033–43.
[7] Currier SC, Lee CK, Chang BS, et al. Mutations in POMT1 are found in a minority of patients with Walker–Warburg syndrome. Am J Med Genet A 2005;133A:53–7.
[8] van Reeuwijk J, Brunner HG, van Bokhoven H. Glyc-*O*-genetics of Walker–Warburg syndrome. Clin Genet 2005;67:281–9.
[9] Kim DS, Hayashi YK, Matsumoto H, et al. POMT1 mutation results in defective glycosylation and loss of laminin-binding activity in alpha-DG. Neurology 2004;62:1009–11.
[10] van Reeuwijk J, Janssen M, van den Elzen C, et al. POMT2 mutations cause alpha-dystroglycan hypoglycosylation and Walker Warburg syndrome. J Med Genet 2005.
[11] Kobayashi K, Nakahori Y, Miyake M, et al. An ancient retrotransposal insertion causes Fukuyama-type congenital muscular dystrophy. Nature 1998;394:388–92.
[12] Longman C, Brockington M, Torelli S, et al. Mutations in the human LARGE gene cause MDC1D, a novel form of congenital muscular dystrophy with severe mental retardation and abnormal glycosylation of α-dystroglycan. Hum Mol Genet 2003;12:2853–61.
[13] van Reeuwijk J, Grewal PK, Salih MA, et al. Intragenic deletion in the LARGE gene causes Walker–Warburg syndrome. Hum Genet 2007;121:685–90.
[14] Quijano-Roy S, Marti-Carrera I, Makri S, et al. Brain MRI abnormalities in muscular dystrophy due to FKRP mutations. Brain Dev 2006;28:232–42.
[15] Louhichi N, Triki C, Quijano-Roy S, et al. New FKRP mutations causing congenital muscular dystrophy associated with mental retardation and central nervous system abnormalities. Identification of a founder mutation in Tunisian families. Neurogenetics 2004;5:27–34.
[16] Topaloglu H, Brockington M, Yuva Y, et al. FKRP gene mutations cause congenital muscular dystrophy, mental retardation, and cerebellar cysts. Neurology 2003;60:988–92.
[17] Mercuri E, Topaloglu H, Brockington M, et al. Spectrum of brain changes in patients with congenital muscular dystrophy and FKRP gene mutations. Arch Neurol 2006;63:251–7.
[18] Beltran-Valero de Bernabe D, Voit T, Longman C, et al. Mutations in the FKRP gene can cause muscle–eye–brain disease and Walker–Warburg syndrome. J Med Genet 2004;41:e61.
[19] Biancheri R, Bertini E, Falace A, et al. POMGnT1 mutations in congenital muscular dystrophy: genotype–phenotype correlation and expanded clinical spectrum. Arch Neurol 2006;63:1491–5.
[20] D'Amico A, Tessa A, Bruno C, et al. Expanding the clinical spectrum of POMT1 phenotype. Neurology 2006;66:1564–7, discussion 1461.
[21] Balci B, Uyanik G, Dincer P, et al. An autosomal recessive limb girdle muscular dystrophy (LGMD2) with mild mental retardation is allelic to Walker–Warburg syndrome (WWS) caused by a mutation in the POMT1 gene. Neuromuscul Disord 2005;15:271–5.
[22] van Reeuwijk J, Maugenre S, van den Elzen C, et al. The expanding phenotype of POMT1 mutations: from Walker–Warburg syndrome to congenital muscular dystrophy, microcephaly, and mental retardation. Hum Mutat 2006;27:453–9.
[23] Yanagisawa A, Bouchet C, Van den Bergh PYK et al. New POMT2 mutations causing congenital muscular dystrophy: identification of a founder mutation. Neurology 2007, in press.
[24] Manya H, Sakai K, Kobayashi K, et al. Loss-of-function of an *N*-acetylglucosaminyltransferase, POMGnT1, in muscle–eye–brain disease. Biochem Biophys Res Commun 2003;306:93–7.
[25] Vajsar J, Zhang W, Dobyns WB, et al. Carriers and patients with muscle–eye–brain disease can be rapidly diagnosed by enzymatic analysis of fibroblasts and lymphoblasts. Neuromuscul Disord 2006;16:132–6.
[26] Akasaka-Manya K, Manya H, Endo T. Mutations of the POMT1 gene found in patients with Walker–Warburg syndrome lead to a defect of protein *O*-mannosylation. Biochem Biophys Res Commun 2004;325:75–9.
[27] Manya H, Chiba A, Yoshida A, et al. Demonstration of mammalian protein *O*-mannosyltransferase activity: coexpression of POMT1 and POMT2 required for enzymatic activity. Proc Natl Acad Sci USA 2004;101:500–5.
[28] Taniguchi K, Kobayashi K, Saito K, et al. Worldwide distribution and broader clinical spectrum of muscle–eye–brain disease. Hum Mol Genet 2003;12:527–34.
[29] Zhang W, Vajsar J, Cao P, et al. Enzymatic diagnostic test for muscle–eye–brain type congenital muscular dystrophy using commercially available reagents. Clin Biochem 2003;36:339–44.
[30] Mercuri E, D'Amico A, Tessa A, et al. POMT2 mutation in a patient with 'MEB-like' phenotype. Neuromuscul Disord 2006;16:446–8.
[31] Xiong H, Kobayashi K, Tachikawa M, et al. Molecular interaction between fukutin and POMGnT1 in the glycosylation pathway of alpha-dystroglycan. Biochem Biophys Res Commun 2006;350:935–41.
[32] Zhang J, Wang Y, Chu Y, et al. Agrin is involved in lymphocytes activation that is mediated by alpha-dystroglycan. FASEB J 2006;20:50–8.